Effect of Ag content in ZnO-Ag nanocomposites prepared by spray pyrolysis method for degradation of textile dye waste

Cite as: AIP Conference Proceedings **2219**, 030005 (2020); https://doi.org/10.1063/5.0003058
Published Online: 05 May 2020

Tantular Nurtono, Timotius Candra Kusuma, Meditha Hudandini, et al.

Effect of Ag Content in ZnO-Ag Nanocomposites Prepared by Spray Pyrolysis Method for Degradation of Textile Dye Waste

Tantular Nurtono[1], Timotius Candra Kusuma[1], Meditha Hudandini[1], Widiyastuti Widiyastuti[1], Manabu Shimada[2], Suci Madhania[1], Siti Machmudah[1], Dewi Puspitasari[1], Sugeng Winardi[1] and Kusdianto Kusdianto[1, a)]

[1]*Department of Chemical Engineering, Institut Teknologi Sepuluh Nopember (ITS), Sukolilo, Kampus ITS Sukolilo, Surabaya 60111, Indonesia.*
[2]*Department of Chemical Engineering, Graduate School of Engineering, Hiroshima University, 4-1, Kagamiyama 1-chome, Higashi-Hiroshima, Hiroshima 739-8527, Japan.*

[a)]Corresponding author: kusdianto@chem-eng.its.ac.id

Abstract. In this study, ZnO-Ag nanocomposites with different Ag loadings have been successfully synthesized by spray pyrolysis using nitrogen as a carrier gas. The Ag loading with various concentrations from 0 to 10 %wt was doped to the ZnO particles. The performance of products, ZnO-Ag nanocomposites, was subsequently tested by measuring the photocatalytic degradation of organic waste from the textile dye. Morphology, crystallite size and crystalline phase, surface area and functional group of hydroxyl of the produced nanocomposites were characterized by scanning electron microscopy (SEM), X-ray diffraction (XRD), Brunauer–Emmett–Teller (BET) and Fourier Transform Infrared Spectroscopy (FTIR), respectively. SEM images indicated that the average particle size of the nanocomposite measured by ImageJ software increased with increasing Ag loading. The average size of nanocomposite with Ag loading at 0, 1, 5, and 10 %wt were 784, 850, 856 and 954 nm, respectively. The XRD results detected the existence of Ag in ZnO-Ag nanocomposite. However, the addition of Ag in the nanocomposite did not alter the crystallite size significantly, where the crystallite size was found approximately around 18 to 57 nm. Moreover, BET analysis showed the increase of specific surface area with increasing Ag content in exception for Ag content at 5 %wt. Finally, ultraviolet (UV) light was used as an irradiation source to evaluate the performance of photocatalytic degradation of textile-dye-waste from the textile industry in Gresik-Indonesia. The results showed that Ag loading at 5 %wt produced the highest degradation efficiency among the other concentrations including the pristine ZnO. This research resulted in a simple and effective route for fabricating ZnO-Ag nanocomposite; therefore, it can be considered as a potential candidate for the direct application in degradation of textile-dye-waste.

INTRODUCTION

Textile-dye-waste is a hazardous waste because it is toxic and mutagenic. Furthermore, it can also reduce the penetration of light into the water [1] resulting the decrease in the photosynthetic activity of aquatic plants. It will cause a lack of oxygen for the animals and plants in the ecosystem. Due to this reason, the organic pollutant derived from textile-dye-waste should be properly treated. There are several ways to degrade organic waste. Conventional methods are widely used for degradation of textile-dye-waste via flocculation, membrane filtration, ion exchange, adsorption, electrochemical oxidation and so on. However, these methods have disadvantages such as sludge production, sludge disposal, not suitable for all dyes, transfer contaminants, and cost of electricity, respectively [2]. Moreover, using conventional methods do not convert the textile-dye-waste into different compounds that are environmentally friendly, since they just alter to another form which requires further processing.

Recently, bio-degradation method using cyanobacteria is able to degrade the organic waste but it is time-consuming [1], because it requires 14 days to degrade the waste. Moreover, the efficiency of degradation is also

2nd International Conference and Exhibition on Powder Technology (ICePTi) 2019
AIP Conf. Proc. 2219, 030005-1–030005-10; https://doi.org/10.1063/5.0003058
Published by AIP Publishing. 978-0-7354-1975-9/$30.00

significantly affected by several conditions, such as anaerobic or aerobic process. Photodegradation method is then used as the most promising method to degrade the textile-dye-waste, since the rate of degradation is much faster than bio-degradation method. The mechanism used for photodegradation is based on the usage semiconductor materials after irradiation with photon energy from lights, where ZnO is the most widely developed as a catalyst material [3-5]. Generally, the photocatalytic process occurs when the photon energy from a light source exceeds the bandgap energy of ZnO so that electrons in the valence band (VB) will be excited to the conduction band (CB) and leave holes in VB. The formed holes will react with water or hydroxyl groups to form hydroxyl radicals. These hydroxyl radicals are able to degrade textile-dye-waste. Unfortunately, the generated holes in the VB will join immediately with the produced electrons in resulting the decrease of photocatalytic performance, which is commonly called as electron-hole recombination [6].

Several studies have been conducted to increase the photocatalytic activity of ZnO by adding various materials such as: tourmaline [7], graphene [8], TiO_2 [9], and noble metals with Ag [10, 11], Pt [12], Au [13]. It is reported that the addition of Ag metal will enhance the photocatalytic activity as much as 34 % greater than using pristine material [6, 10] because the excited electrons will be trapped by Ag nanoparticles. The existence of Ag nanoparticle is able to prevent electron-hole recombination.

There are several methods to fabricate the ZnO-Ag nanocomposite materials, such as: sol-gel, precipitation, electrodeposition, hydrothermal and solvothermal. However, these processes have the disadvantage which requires a large number of processing steps and then require further steps to remove residue or impurities. In our previous study, we have successfully fabricated ZnO-Ag nanocomposite with flame pyrolysis [10], where the best photocatalytic performance was obtained at 5 %wt Ag loading. Unfortunately, controlling temperature inside the flame reactor was quite difficult. In this study, ZnO-Ag is synthesized using the spray pyrolysis method which the temperature inside the tubular reactor is more controllable. It is because the heating media used in a spray tubular furnace is from electricity source. It makes that the temperature in the tubular reactor can be maintained properly. In the previous study, ZnO-Ag nanocomposite was prepared by spray pyrolysis using air as a carrier gas [14], where air consists of 79 % moles of nitrogen (N_2) and 21 % moles of oxygen (O_2). In this study, N_2 is used as a carrier gas. The objective of this study is then to investigate the effect of Ag loading on the photocatalytic performance of ZnO-Ag nanocomposite synthesized by spray pyrolysis under N_2 as the carrier gas. The organic pollutant used for photocatalytic test is from UD. ATBM Jufri Hartono Gresik East Java. Photocatalytic activity is expressed by measuring percent degradation and rate constant under UV light irradiation.

MATERIALS AND METHOD

Materials used in this study included zinc acetate dehydrate crystals ($Zn(CH_3COO)_2.2H_2O$) 99.5% (E. Merck, D-6100 Darmstadt, FR Germany), silver nitrate ($AgNO_3$) crystals 99.5% (E. Merck, D-6100 Darmstadt, FR Germany), distilled water as dispersing media, and pure nitrogen as a carrier gas (Samator, purity 99%).

Initially, the zinc acetate dehydrate crystal was dispersed into the distilled water using a sonicator to produce homogeneous zinc acetate-water mixture with a concentration of 0.1 M. Silver nitrate with various loadings from 0 to 10 %wt based on percent weight of zinc acetate was then added to the zinc acetate-water mixture under sonication for 15 min to form a homogeneous dispersion. 40 mL of the prepared precursor was subsequently poured to the ultrasonic nebulizer (Omron, NE-U17). The fresh precursor was also continuously flowed to an ultrasonic nebulizer using a peristaltic pump (Eyela Micro Tube Pump MP-3N) to keep the volume in the ultrasonic nebulizer constant. By using this system, it is expected that the precursor concentration inside the nebulizer is also constant during nebulizing. Ultrasonic nebulizer was used as droplet production. The generated droplets were then sprayed into the tubular furnace reactor using nitrogen as a carrier gas with a flow rate of 2 LPM which was regulated by a flowmeter (Cole Parmer). Tubular furnace operated at 100 V and 600 W was used as heat sources. The temperature in the tubular furnace was set constant at 400 ºC. The nanocomposites formed in the tubular reactor will be moved towards the electrostatic precipitator (EP, homemade) connected to DC high voltage at 40 kV. The generated particles will be captured in this part. The temperature of electrostatic precipitator was kept constant as high as 120 ºC to prevent condensation caused by evaporation of water solvent. While incondensable gas and uncaptured particles will be flowed into the water trap. The schematic image of experimental setup can be seen in Fig. 1.

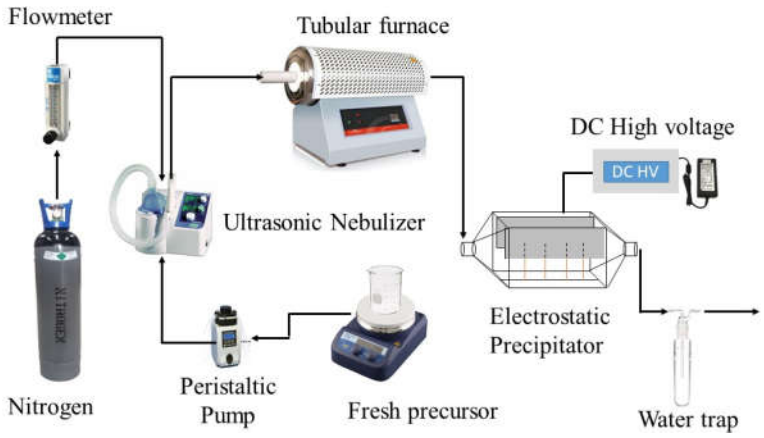

FIGURE 1. A schematic image of the fabrication method of ZnO-Ag nanocomposites by spray pyrolysis

The obtained products were characterized using scanning electron microscopy (SEM, FlexSEM1000, Hitachi High Technologies), X-ray diffraction (XRD, Philip XPERT MPD), BET surface area (Quantachrome NovaWin), Fourier transform infrared spectroscopy (Shimadzu) to observe the morphology, crystallinity and crystallite phase, surface area, and functional group of hydroxide, respectively. The XRD measurements were carried out using an accelerating voltage of 40 kV and 30 mA, the initial position of 2 thetas at 10 º and the final position at 80º, the step size at 0.017º, and the scan step time of 10.15 s. Photocatalytic performance was evaluated by monitoring the degradation of dye-textile-waste (UD. ATBM Jufri Hartono) with UV–visible spectrometer (Thermo Scientific Genesys 10s). The photon energy used for photocatalytic test was from UV lamp (20 W x 2). The concentration of dye-textile-waste was determined by measuring the UV absorbance at a wavelength of 376 nm.

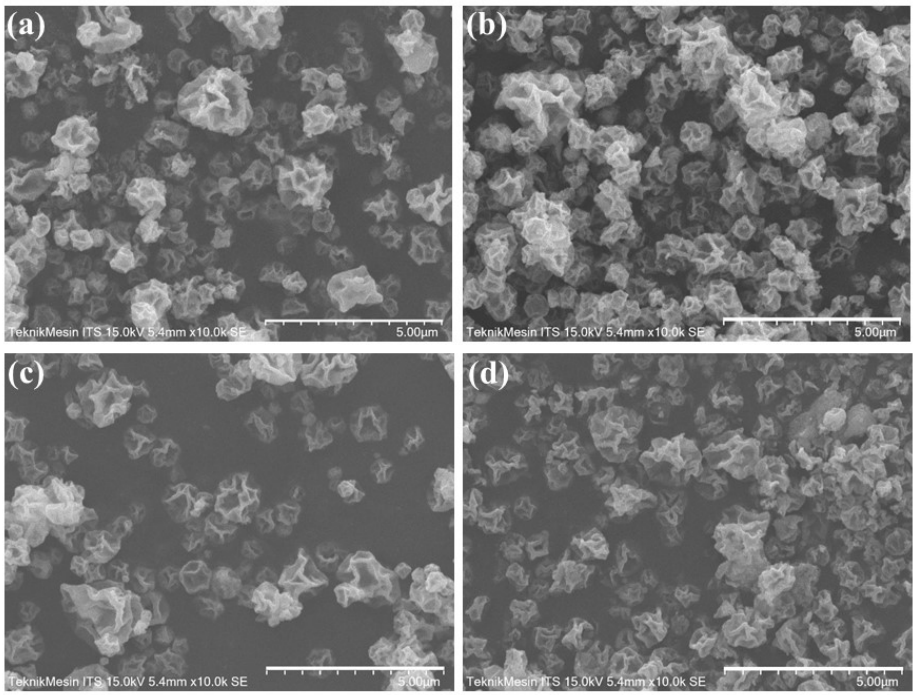

FIGURE 2. SEM images of ZnO-Ag nanocomposites prepared by spray pyrolysis at different Ag loading levels at (a) 0 %, (b) 1 %, (c) 5 % and (d) 10 %wt

RESULTS AND DISCUSSION

SEM Analysis

Figure 2 depicts scanning electron microscopy images of ZnO-Ag nanocomposites for various Ag loading in the range of 0 to 10 %wt. The morphology of the obtained products is sphere-like structures assembled with interwoven nanoplate and showing similar morphology for all samples with various Ag loadings. This result shows a similar tendency with previous research [15] which states that this morphology of the produced nanocomposites caused by to the low precursor concentration and low decomposition reaction temperature. However, discussion about this phenomenon reported by previous study is limited. In our opinion, decomposition reaction temperature in spray pyrolysis refers to the residence time of droplets in the heating region. Another important part is the nucleation step and growth mechanism. When the decomposition reaction temperature is high, the supersaturation rate and flow of particles are assumed to be high. Higher supersaturation degree generates higher nucleation rates, while higher movement increases the contact rates and growth rates of individual particles. For low temperatures, the driving force of the reaction in the system and nucleation rates are low. Therefore, the nucleation that already formed in the previous step will grow immediately.

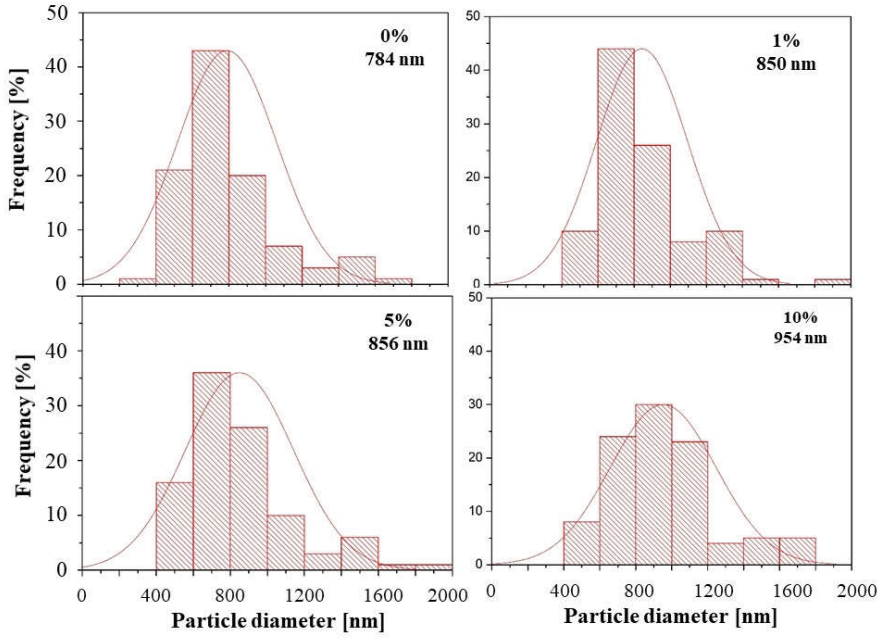

FIGURE 3. Particle size distribution of the ZnO-Ag nanocomposite estimated by measurement of the particle sizes using imageJ at different Ag content (a) 0 %, (b) 1 %, (c) 5 % and (d) 10 %

ImageJ software was used as a measurement tool for estimating the particle size distribution by measuring several hundreds of particles based on SEM images as depicted in Fig. 3. It can be obviously observed that the average particle size increases with an increase of Ag loading, with the largest size of nanocomposites found at 10% Ag loading. This is in accordance with our previous research [6], which is attributed due to metal-induced crystallization phenomenon and the fusion of particles.

Effect of Silver Loading on Average Crystallite Size and Specific Surface Area

The results of the XRD patterns as shown in Fig. 4 match with the Joint Committee on Powder Diffraction Standards (JCPDS) ZnO data (file no. 98-005-7478) and JCPDS Ag (file no. 04-0783). In the JCPDS ZnO data, there are 7 peaks at 31.77°, 34.44°, 36.26°, 47.55°, 56.59°, 62.86° and 67.94°. Whereas in the JCPDS Ag data there are 4

peaks at 38.06°, 44.24°, 64.34°, and 77.22°. As can be seen from Fig. 4, the obtained results for pristine ZnO also have 7 similar peaks at 31.58°, 33.82°, 35.93°, 47.10°, 56.47°, 62.40° and 67.84° and correspond to the ZnO phase planes (1 0 0), (0 0 2), (1 0 1), (1 0 2), (1 1 0), (1 0 3), and (1 1 2) respectively. It can be concluded that the nanocomposites formed are ZnO without any impurities. The crystal phase of ZnO can be considered as hexagonal wurtzite [16]. The presence of Ag in nanocomposites can be identified by the existing XRD peaks at 37.82° (1 1 1) and 77.00° (3 1 1). These peaks correspond to crystal structure plane of Ag as face-centered cubic (FCC).

Unexpectedly, the addition peak at 43.58° can be seen in Fig. 4 when the concentration of Ag loading as much as 1 and 5 %wt. These peaks may be ascribed due to the presence of Zn in the nanocomposite according to the JCPDS of Zn data (file no 4-831). The possibility of this phenomenon is considered by incomplete oxidation process due to the absence of oxygen as a carrier gas. Some of zinc may be not completely converted to ZnO because the reaction of ZnO formation is influenced by the presence of oxygen. However, ZnO have been completely formed when 10% Ag loading was used. This may be caused by an adequate source of oxygen from the decomposition reaction of silver nitrate. Unfortunately, the Zn peak also disappears from the XRD peak at the pristine ZnO. At this moment, we cannot explain in details this phenomenon and addition experiments should be conducted in the future.

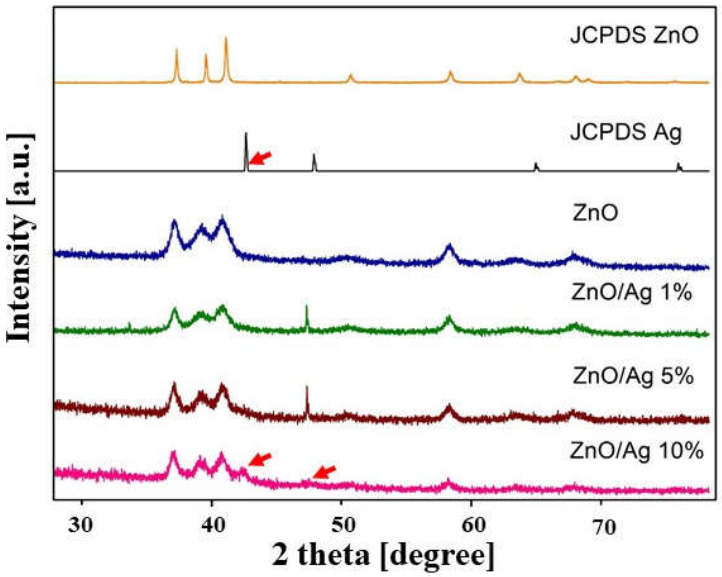

FIGURE 4. XRD patterns of ZnO-Ag nanocomposites with different Ag loadings

The average crystallite size of nanocomposites (D) was determined based on the broadening XRD peak (FWHM) using the Scherrer equation.

$$D = \frac{k\,\lambda}{B\cos\theta} \tag{1}$$

Here, k and λ are the constants, where the value of k is 0.94 and CuKα radiation source (λ) is = 0.15418 nm. While, B is full-width at half-maximum (FWHM) suitable to XRD peaks, and θ (theta) is a half the angle of the peak. Based on the calculation using Eq. (1), the crystallite size of ZnO-Ag with various Ag loadings can be seen in Table 1. From these results, it can be concluded that the smallest crystallite size and the largest surface area were found at 10 %wt Ag loading. Since the variation value of the crystallite size is a matter of just a few nm, it can be assumed that such a variation may have a less significant result on photocatalytic performance.

TABLE 1. Crystallite size, specific surface area, and area of hydroxyl of ZnO-Ag nanocomposites with differing Ag loadings

Variables (% Ag loading)	Crystallite size (nm)	Specific surface area (m^2/g)	OH area (cm^2)
0	20.26	237.8	8584
1	57.2	227.9	6880
5	38.6	97.9	5728
10	18.43	932.7	5881

FTIR Analysis of ZnO-Ag Nanocomposites

Figure 5 shows the FTIR spectra of ZnO-Ag at 5 %wt conducted in the range of wave number at 4000 to 400 cm^{-1}. The peak between 400 – 750 cm^{-1} corresponds the ZnO bond, while the peak in the range 900 – 1500 cm^{-1} represents to the presence of oxygen stretching and bending. The evidence that water adsorption occurs in the product can be seen by the appearance of a strong band near 1550 – 1580 cm^{-1} which corresponds to H-O-H bending vibration mode. Finally, the existence of hydroxyl group in the nanocomposite can be identified by showing the band at 3200 – 3700 cm^{-1}. Later, we believe that these functional groups will react with catalyst material to produce hydroxyl radicals [17]. The simple quantitative analysis was used by measuring the area under hydroxyl group peak to compare the existence of hydroxyl group in each nanocomposite as shown in Table 1. Theoretically, the larger area should produce higher number of the hydroxyl radicals. Table 1 indicates that the largest peak area is found when the pristine ZnO was used which may be caused by to the possibility of agglomeration.

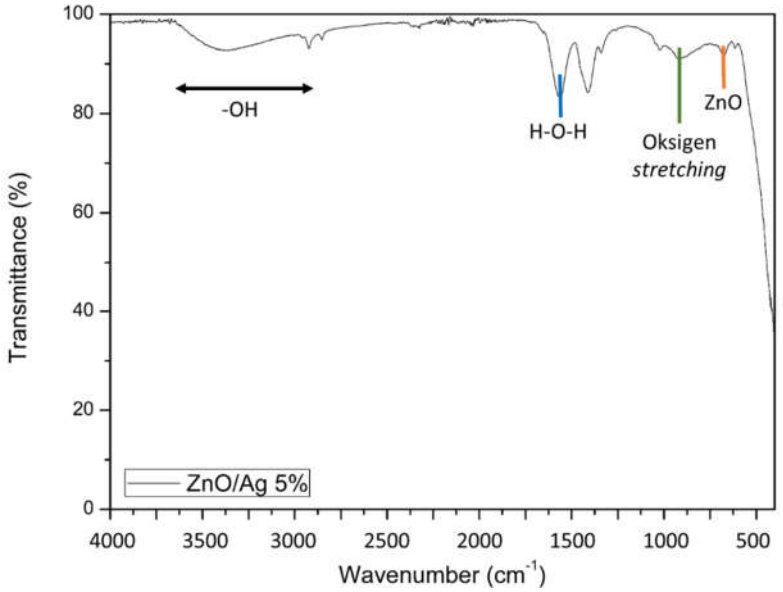

FIGURE 5. Functional group of the produced nanocomposite at 5 %wt analyzed by FTIR

Photocatalytic Activity

Degradation of textile-dye-waste for ZnO-Ag nanocomposites with different Ag loadings can be seen in Fig. 6. This result is calculated based on equation (2), where C_0 and C_t represent the initial concentration and concentration at certain irradiation time (t), respectively. UV-Vis spectroscopy was conducted to measure the absorbance of the samples to determine the textile-dye-waste degradation efficiency. The obtained absorbance is then converted to concentration according to Lambert-Beer law, where the absorbance of a sample is equivalent to its concentration.

$$The\ textile\ dye\ waste\ degradation\ efficiency\ = \frac{C_0 - C_t}{C_0}\ x\ 100\% \qquad (2)$$

The photodegradation test was started by placing the samples inside dark condition for 30 min under vigorous agitation to allow equilibrium of adsorption and desorption from nanocomposites. From Fig. 6, the highest degradation efficiency is obtained at Ag loading as much as 5 %wt. Whereas the lowest adsorption activity is found at the 10 %wt. This is because the higher concentration of Ag will block the incoming light to the ZnO particle [10]. The percentage degradation of pristine ZnO and Ag loading at 1, 5, and 10 %wt are 22 %, 41 %, 50 % and 7 %, respectively. It can be obviously observed from Fig. 6 that the addition of Ag loading can enhance the photocatalytic activity. However, the degradation of textile-dye-waste decreases when the Ag loading is greater than 5 %wt. According to Liu et al. [18], decreasing the degradation efficiency at higher content of Ag can be ascribed to the light penetration to ZnO is reduced due to obstruction by Ag nanoparticles embedded in the surface of ZnO. This result is also in a good agreement with reported by our previous study, the best degradation efficiency was obtained at 5 %wt using ZnO-Ag prepared by flame pyrolysis [10].

The photocatalytic performance can also be identified by estimating the constant rate (k) that is considered as a pseudo-first order with the following equation:

$$-ln\left(\frac{C_t}{C_0}\right) = kt \tag{3}$$

The photocatalytic rate constants for each variable were obtained for pristine ZnO, 1%, 5%, and 10% Ag loading are 0.0025, 0.0036, 0.0059, and 0.0007 min^{-1}, respectively. It can be clearly observed in Fig. 7 that Ag loading at 5 %wt shows the best photocatalytic performance.

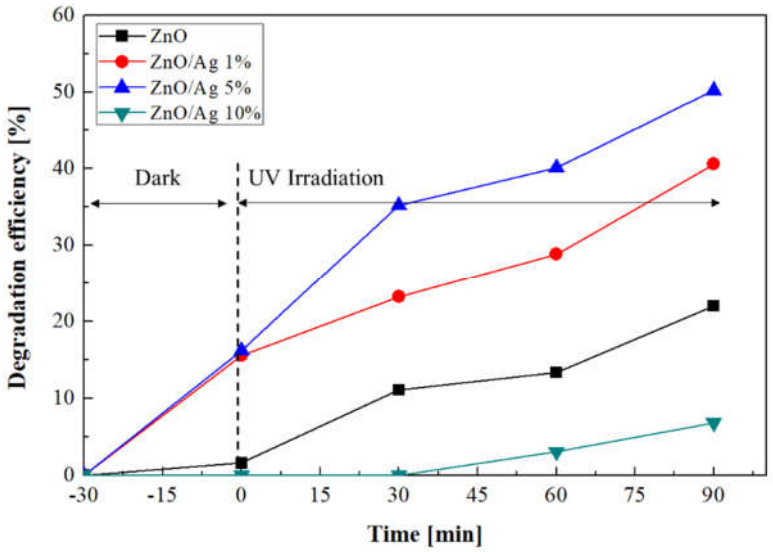

FIGURE 6. Textile dye degradation efficiency of ZnO-Ag nanocomposite with different Ag loadings versus irradiation time.

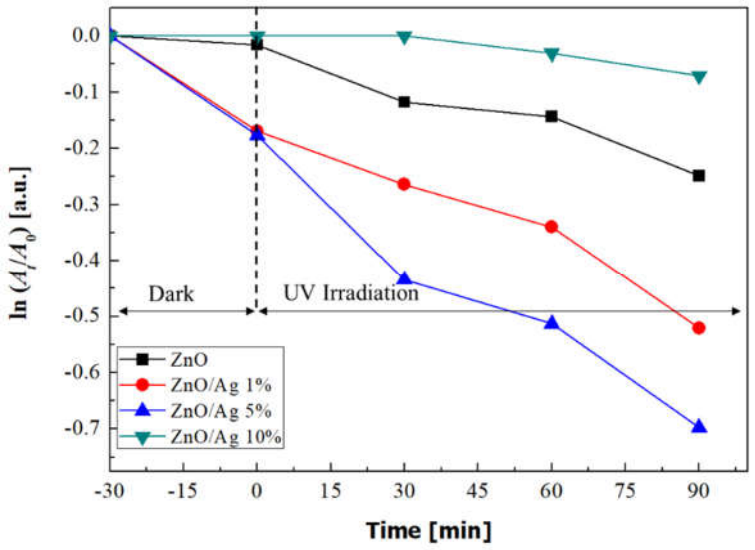

FIGURE 7. Plots of ln C_t/C_0 vs irradiation time of the ZnO-Ag nanocomposites with various Ag loadings

Proposed Mechanism of Adsorption and Photocatalytic Activity

Figure 8 explains the mechanism of adsorption of textile-dye-waste with Ag-doped to ZnO nanocomposites. The waste used is direct orange S (DOS) with the molecular formula $C_{33}H_{22}N_6Na_2O_9S_2$. In the form of a solution, it will be ionized into positive ions (Na^+) and negative ion ($C_{33}H_{22}N_6O_9S_2^{2-}$). While nanocomposites will act as positively charged metal oxides. Hence, there is an attractive force between negative and positive ion. It causes some textile dye molecules to stick to the surface of the nanocomposites and the concentration of textile dye waste decreases due to adsorption process.

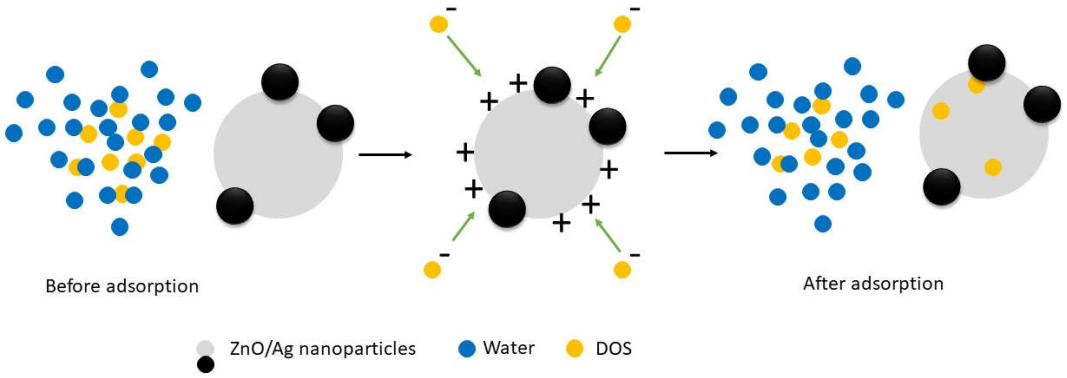

FIGURE 8. Illustration of the proposed mechanism of adsorption activity of ZnO-Ag nanocomposites with various Ag content levels under dark conditions

While the mechanism for the photocatalytic is totally difference with adsorption process. As shown in Fig. 9, it explains how the photocatalyst of the nanocomposites induced by ultraviolet light with the photon energy is greater than or equal to the bandgap energy of zinc oxide. The photon energy from ultraviolet light excites the electron (*e*-) from the valance band (VB) of zinc oxide to the conduction band (CB) and produces a hole (h^+). For the Ag-doped to ZnO nanocomposites, the produced electrons were trapped in the Ag nanoparticle, where electron-hole recombination is inhibited due to the Fermi energy level of the Ag-doped to ZnO. The produced holes can react with water or hydroxyl groups resulting in hydroxyl radical species that can react and degrade the dye-textile-waste solution [17].

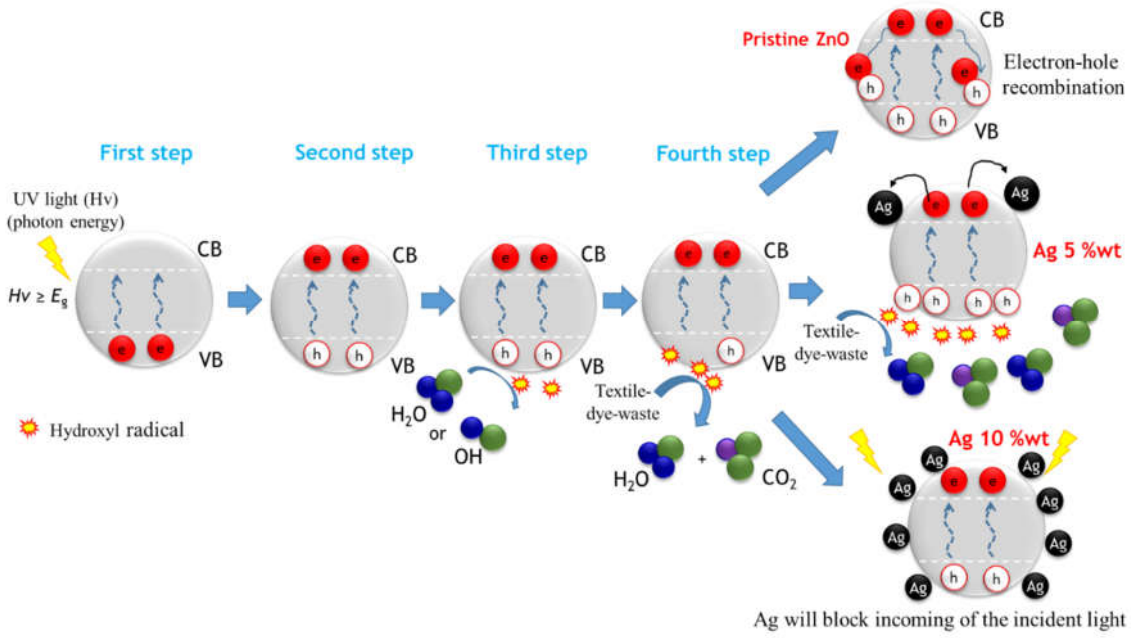

FIGURE 9. Illustration of the proposed mechanism of photocatalytic activity of ZnO-Ag nanocomposites with various Ag content levels under UV light irradiation

CONCLUSIONS

The ZnO-Ag nanocomposite was successfully synthesized using spray pyrolysis using nitrogen as a carrier gas. The nanocomposite formed was characterized by SEM, XRD, BET, FTIR, and UV-Vis spectroscopy. SEM results showed that the morphology of nanocomposites was sphere-like structures assembled with interwoven nanoplates. The nanocomposite produced was in the nanometer range, with the largest size was observed at 10 %wt with a size of 955 nm. XRD indicated that the crystalline phase structure of the pristine ZnO was hexagonal wurtzite. The presence of Ag can be detected by XRD on variable nanocomposites of 10 %wt Ag loading. The smallest crystallite size (18 nm) and the largest specific surface area (932 cm^2) were found in nanocomposites at 10 %wt. The best degradation efficiency of textile-dye-waste was observed when the Ag content as much as 5 %wt with value was 50.2 %. Photocatalytic activity was also investigated by measuring the rate constant under irradiation with UV light, where the highest rate constant was found as 0.0059 min^{-1}. Increasing the Ag content up to 10 %wt reduced the photocatalytic performance. We believe that our research will be valuable as a reference for ZnO-Ag nanocomposite fabrication research in the future to degrade the textile-industry-wastes.

ACKNOWLEDGMENTS

The authors are grateful to UD. ATBM Jufri Hartono for providing the textile-dye-waste. This work was financially supported by the Lembaga Penelitian dan Pengabdian Masyarakat (LPPM) ITS with scheme “Abdimas Berbasis Penelitian Dana Lokal ITS 2019” under contract number 1342/PKS/ITS/2019.

REFERENCES

1. P. M. Dellamatrice, M. E. Silva-Stenico, L. A. B. Moraes, M. F. Fiore and R. T. R. Monteiro, Brazilian J. Microbiol. **48**, 25–31 (2017).
2. C. D. Raman and S. Kanmani, J. Environ. Manag. **177**, 341–355 (2016).
3. H. Sutanto, I. Nurhasanah and E. Hidayanto, Mat. Sci. Forum. **827**, 3–6 (2015).

4. M. Karyaoui, A. Mhamdi, H. Kaouach, A. Labidi, A. Boukhachem, K. Boubaker, M. Amlouk and R. Chtourou, Sci. Semicond. Process. **30**, 255–262 (2015).
5. S. I. Inamdar, V. V. Ganbavle and K. Y. Rajpure, Superlattices Microstruct. **76**, 253–263 (2014).
6. K. Kusdianto, D. Jiang, M. Kubo and M. Shimada, Ceram. Int. **43**, 5351–5355 (2017).
7. C. Yu, Z. Tong, S. Li and Y. Yin, Mat. Lett. **240**, 161–164 (2019).
8. R. Cai, J. Wu, L. Sun, Y. Liu, T. Fang, S. Zhu, S. Li, Y. Wang, L. Guo, C. Zhao and A. Wei, Mat. Design. **90**, 839–844 (2016).
9. R. Qin, F. Meng, M. W. Khan, B. Yu, H. Li, Z. Fan and J. Gong, Mat. Lett. **240**, 84–87 (2019).
10. K. Kusdianto, W. Widiyastuti, M. Shimada, T. Nurtono, S. Machmudah and S. Winardi, Int. J. Tech. **10**(3), 571–581 (2019).
11. H. Sudrajat and S. Babel, Optik. **183**, 472–482 (2019).
12. M. Zayed, A. M. Ahmed and M. Shaban, Int. J. Hydrogen. Energ. **44**, 17630–17648 (2019).
13. T. K. Pathak, R. E. Kroom and H. C. Swart, *Vacuum*. **157**, 508–513 (2018).
14. K. B. Dermenci, B. Genc, B. Ebin, T. Olmez-Hanci and S. Gürmen, J. Alloys. Compound. **586**, 267–273 (2014).
15. E. Emil, G. Alkan, S. Gürmen, R. Rudolf, D. Jenko and B. Friedrich, Metals **8**, 569–580 (2018).
16. G. Nagaraju, U. Udayabhanu, S. Shivaraj, S. A. Prashanth, M. Shastri, K. V. Yathish, C. Anupama and D. Rangappa, Mat. Res. Bulletin. **94**, 54–63 (2017).
17. C. Cheng, A. Amini, C. Zhu, Z. Xu, H. Song and N. Wang, Sci. Rep. **4**, 4181 (2014).
18. Y. Liu, Q. Zhang, M. Xu, H. Yuan, Y. Chen, J. Zhang, K. Luo and B. You, App. Surface Sci. **476**, 632–640 (2019).